

Bending strength and effective modulus of atmospheric ice

Majid Kermani ^{a,*}, Masoud Farzaneh ^{a,1}, Robert Gagnon ^{b,2}

^a *Industrial Chair on Atmospheric Icing of Power Network Equipment (CIGELE) and Canada Research Chair on Atmospheric Icing Engineering of Power Networks (INGIVRE) at Université du Québec à Chicoutimi, Québec, Canada*

^b *Institute for Ocean Technology, National Research Council of Canada, St. John's, Canada*

Received 11 June 2007; accepted 23 August 2007

Abstract

Bending strength and the effective modulus of atmospheric ice accumulated in a closed loop wind tunnel at temperatures -6°C , -10°C and -20°C with a liquid water content of 2.5 g/m^3 have been studied at different strain rates. More than 120 tests have been conducted. Ice samples, accumulated at each temperature, have been tested at the accumulation temperature. In addition, tests have been performed at temperatures of -3°C and -20°C , for the ice accumulated at -10°C . These tests showed a clear dependency of bending strength of atmospheric ice on test temperature at low strain rates. Strain rate effects are implied because the spread in bending strength for the different temperatures diminishes as strain rate increases. The results also reveal that, in most cases, the effective modulus of atmospheric ice increases with increasing strain rate. The bending strength of atmospheric ice accumulated at -10°C has been found to be greater than that of ice accumulated at -6°C and -20°C . The results show that the effective modulus of ice accumulated at -20°C at higher strain rates is less than that of the two other types.

© 2007 Elsevier B.V. All rights reserved.

Keywords: Atmospheric ice; Beam; Bending strength; Effective modulus

1. Introduction

One of the most important causes for the increase in vulnerability of a power transmission network in cold climate regions is atmospheric ice accretion on ground wires and phase conductors. Atmospheric ice is the result of supercooled water droplets in the atmosphere impinging on exposed surfaces. Basic understanding of the mechanical properties and behaviour of atmospheric ice

has potential applications in many fields such as de-icing techniques to remove ice from wires and conductors and the effects of the resulting transient forces on power network elements.

One of the few studies on the mechanical properties of atmospheric ice is the research of Druez et al. (1986) on compressive strength of ice. In their study, ice accumulated at various air temperatures and air speeds was tested at the same temperature as it had been accumulated. The liquid water content (LWC) of the air flow was set at 0.4 g/m^3 and 0.8 g/m^3 . The mean volume droplet diameter for these two values of LWC was set at $20\text{ }\mu\text{m}$ and $40\text{ }\mu\text{m}$, respectively. Also, two strain rates were used for strength tests, and several wind velocities for the ice accumulation. Druez et al. (1989) also measured the tensile strength of atmospheric ice

* Corresponding author. Fax: +418 5455032.

E-mail addresses: mkermani@uqac.ca (M. Kermani),
Masoud.Farzaneh@uqac.ca (M. Farzaneh),
Robert.Gagnon@nrc-cnrc.gc.ca (R. Gagnon).

URL: <http://www.cigele.ca> (M. Farzaneh).

¹ Fax: +418 5455032.

² Fax: +709 772 2462.

accumulated at temperatures ranging from $-3\text{ }^{\circ}\text{C}$ to $-20\text{ }^{\circ}\text{C}$ where the LWC was set at 0.8 g/m^3 and 1.2 g/m^3 and the droplet diameter for these two values of LWC was set at $40\text{ }\mu\text{m}$.

In contrast to the few studies on atmospheric ice, the flexural strength of other types of ice has been studied by many investigators. For example, Timco and Frederking (1982) performed a series of cantilever beam tests on freshwater ice. They confined themselves to testing only S2 ice at a test temperature of $-10\text{ }^{\circ}\text{C}$. Cantilever beam tests were conducted by those authors in the push-down mode, and the simply supported beams were tested isothermally at $-10\text{ }^{\circ}\text{C}$ in both the push-down and pull-up modes. As another example, Frederking and Svec (1985) studied the stress concentration relief at the root of cantilever beams. Their tests were conducted in the top-in-tension mode of fine-grained ice in an outdoor pool at temperatures ranging from $-5\text{ }^{\circ}\text{C}$ to $-20\text{ }^{\circ}\text{C}$. Also, Dempsey et al. (1989) studied the effects of specimen size on the flexural strength and effective modulus of columnar freshwater ice using four-point-bend tests in two sizes. The larger beam thickness and length in one size were almost 1.5 times greater than the corresponding dimensions of the smaller specimen. Considering the differences in the bending results, they concluded that the specimen size can overshadow the results of flexural strength and effective modulus. Gow and Ueda (1988) performed some bending tests with both cantilever and simply-supported beams of freshwater ice sheets. Their tests within the temperature range $-1\text{ }^{\circ}\text{C}$ to $-19\text{ }^{\circ}\text{C}$ revealed that macrocrystalline (S1) and columnar (S2) ice have different flexural characteristics. They ascribed these differences to variations in the size and orientation of the crystals in the ice as well as to the thermal condition of the beams. The results of the above mentioned works were used for comparison with the results of the present study on atmospheric ice.

We could find no report on the bending strength of atmospheric ice in the literature. Lack of comprehensive information about the strength and mechanical properties of atmospheric ice under various loading conditions led to the present study. In this paper, the bending strength and effective modulus of atmospheric ice for various accumulation temperatures and strain rates are investigated.

2. Ice accumulation

The meteorological conditions prevalent during ice formation, such as wind velocity, liquid water content of air, mean volume droplet diameter and air temperature, can influence the structure of atmospheric ice and, consequently, its mechanical properties. Therefore selec-

tion, monitoring and control of the ice accumulation conditions are very important and will be discussed in the following section.

2.1. Ice accumulation equipment

The ice accumulation conditions for this study were created in the CIGELE (Industrial Chair on Atmospheric Icing of Power Network Equipment at Université du Québec à Chicoutimi) atmospheric icing research wind tunnel which is a closed-loop (air-recirculated) low-speed icing wind tunnel. Three main systems inside the wind tunnel, the fan, the refrigeration unit, and the nozzle spray-bar systems were used to simulate icing conditions as those encountered during various icing processes in nature. Air speed and air temperature in the wind tunnel are adjustable with appropriate accuracy. Atmospheric icing processes are simulated by injecting warm water into a cold air stream through nozzles located at the trailing edge of the horizontal spray bar, designed in the shape of a NACA0012 airfoil. The droplet size distribution depends on the combination of air and water pressures and, within a certain range of the temperature, on the flow rate of water in the supply line. The absolute and relative humidity were measured using a humidity probe placed inside a plastic/aluminum fairing specially designed to resist freezing.

Atmospheric ice was grown from supercooled water droplets impinging on a rotating aluminum cylinder 78 mm in diameter and 590 mm in length. It was placed in the middle of the test section where the distance between the spray nozzles and the cylinder was long enough for thermodynamic equilibrium to be reached between the air flow at its highest velocity and the largest droplets.

The cylinder was cleaned with alcohol before ice accumulation and set in place for 2 h while the system was cooling down. After ice accumulation, the accumulated ice was cut with a warm aluminum blade to avoid any mechanical stress that might cause cracks. The resulting ice slices were then carefully prepared using a microtome to avoid crack formation. The guidelines recommended by the IAHR working group on test methods (Schwarz et al., 1981) were used for preparing the specimens. For the purpose of preparing ice samples and thin sections, the microtome was adjusted carefully to prevent any crack formation. Any sample with broken edges was discarded. The position of specimens extracted from the accumulated ice on the cylinder and load direction in mechanical tests are shown in Fig. 1. The average interval between ice accumulation and bending tests was 5 h.

2.2. Ice accumulation conditions

Atmospheric icing usually occurs at temperatures ranging from $-6\text{ }^{\circ}\text{C}$ to $-20\text{ }^{\circ}\text{C}$ (e.g. [Eskandarian, 2005](#), [Mousavi, 2003](#)). Three temperatures $-6\text{ }^{\circ}\text{C}$, $-10\text{ }^{\circ}\text{C}$ and $-20\text{ }^{\circ}\text{C}$ for accumulation of atmospheric ice have been selected in this study to represent warm, medium and cold icing conditions respectively. In the text that follows, by the expression ‘type of atmospheric ice’ we are referring to the ice that was obtained at one of the accumulation temperatures.

During the winter, wind speeds ranging from 5 m/s to 10 m/s typically lead to natural glaze ice formation, therefore a wind speed of 10 m/s was chosen for this study. The air pressure was 1 NACA standard atmosphere at sea level ($P_{\text{st}} = 101.325\text{ kPa}$) and the relative humidity ranged from 0.81% to 0.92%. The liquid water content (LWC) is a function of the difference between the air and water line pressures, air speed and, within a certain range of the temperature, the flow rate of water in the supply line. The LWC for the wind tunnel of CIGELE as a function of these parameters was calibrated by [Karev et al. \(submitted for publication\)](#). During the calibration, the LWC at the test section of the wind tunnel was measured using the accepted standard technique known as the rotating icing cylinder method ([Stallabrass, 1978](#)). The LWC for icing conditions in nature ranges from 0.5 g/m^3 to 10 g/m^3 , which is manageable by the CIGELE wind tunnel. In this study, the LWC of was set at 2.5 g/m^3 and the corresponding air and water pressures at 103.42 kPa and 379.21 kPa, respectively. Readers are referred to [Kermani](#)

[et al. \(2007\)](#) for more details about ice accumulation conditions and experimental equipment.

3. Test conditions and method

The mechanical properties of ice can be influenced by test conditions such as temperature, specimen size, loading rate, failure mode, etc. Considering this, the test conditions have been chosen very carefully in this study.

The specimens in this investigation were accumulated at different temperatures and tested at their accumulation temperatures. Since a typical wintertime temperature in Quebec is $-10\text{ }^{\circ}\text{C}$, the atmospheric ice accumulated at this temperature was tested at three temperatures $-3\text{ }^{\circ}\text{C}$, $-10\text{ }^{\circ}\text{C}$ and $-20\text{ }^{\circ}\text{C}$. The specimens were kept at the test temperature for two hours before each test.

Strain rate is defined in terms of the strain exerted at the bottom of the ice beam. According to beam-bending theory for three-point loading ([Timoshenko, 1968](#)), the strain rate is given by

$$\dot{\epsilon} = 6h\delta/L^2$$

where h is the beam height, δ is the cross-head speed and L is the beam length.

In order to study the effects of strain rate on the flexural strength and effective modulus of atmospheric ice, a wide range of strain rates, from $3 \times 10^{-5}\text{ s}^{-1}$ to $2 \times 10^{-3}\text{ s}^{-1}$, was selected, and for each set of parameters at least five specimens were tested. According to the guidelines recommended by the IAHR working group on test methods ([Schwarz et al., 1981](#)), loading times to failure of the order of 1 s yield satisfactory results. In the present study, this corresponds to a strain rate of $2 \times 10^{-3}\text{ s}^{-1}$.

Bending force was applied using a hydraulic actuator to the middle of the beam, normal to the axis, at various cross-head speeds. The actuator includes a LVDT which measures its displacement. The speed and direction of cross-head movement is controlled by a servovalve. Another LVDT was positioned on the cross head to measure the deflection of the top surface at the middle of the beam as force was applied. The variation of force and displacement as functions of time were recorded at 1000 samples per second for strain rates of more than $3 \times 10^{-5}\text{ s}^{-1}$, and at 500 samples/s for a strain rate of $3 \times 10^{-5}\text{ s}^{-1}$. The variation of force in the load cell was also monitored continuously and the maximum load during the test was recorded. This digitally recorded maximum load was always within $\pm 1\%$ of the peak value and was used in the calculations.

According to [Schwarz et al. \(1981\)](#), for beams of fresh-water ice (which has the closest structure to atmospheric

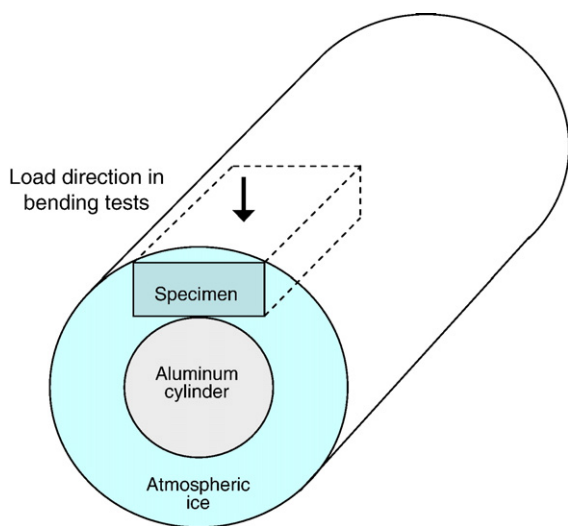


Fig. 1. Schematic illustrating specimen position in accumulated atmospheric ice and loading direction during test.

ice) the ratio of beam width to ice crystal size must be ≥ 10 in order to eliminate the grain size effect. Accordingly, the following dimensions were chosen for our specimens: beam width (w) 40mm, beam thickness (h) 20 mm and beam length (L) 70 mm (Fig. 2).

Tests in which fracture occurred at distances greater than 3 mm from the side of the traverse loading bar (greater than 4.2% of the beam span in Fig. 2) were excluded from the averaged values. Only 8 out of 129 tests had to be discarded for this reason.

The error associated with any particular measurement of bending strength can be determined from the accumulated error associated with all parameters. The uncertainty of F is 0.25%. The error for W and h is that associated with the measurement error of the caliper used to measure the dimensions of the beams and scatter in the measurement, which is 0.01 mm. The uncertainty of measurement of the beam deflection is 0.20%. Therefore, the total uncertainty in any single measurement of the bending strength and the effective modulus is 4.43% and 12.83%, respectively. The inherent scatter in the test results is considerably greater than this. The uncertainty for the failure time is 0.001 second, which corresponds to the time interval of the acquisition rate and the uncertainty of strain rate measurement is 1.68%.

4. Ice characterization

The characteristics (grain structure, air bubble size, porosity, etc.) of these three types of atmospheric ice were studied in Kermani et al. (2007). The average grain size of atmospheric ice accumulated at -6°C is approximately 1.5 mm, and varies from 0.5 mm to 3 mm. The average diameter of the bubbles in this type of atmospheric ice is roughly 0.07 mm, with considerable variation in size according to the limited number of measurements.

The grain size of the atmospheric ice accumulated at -10°C is approximately 0.5 mm which is considerably smaller than that accumulated at -6°C . The average

diameter of bubbles for this type of ice is roughly 0.1 mm, with considerable variation in size according to the limited number of measurements.

The structure of atmospheric ice accumulated at -20°C is quite different from the other two types. A significant number of cavities and cracks are visible in this type of atmospheric ice. The presence of these cavities is attributed to the high freezing rate of the droplets, which prevents them from filling the cavities.

The porosity of this type of atmospheric ice was found to be 8.5% owing to the significant amount of cavities and voids. According to the measurements of sample mass and volume, the porosity of the ice accumulated at -6°C and -10°C were approximately the same (2.9%). The more cloudy appearance of the ice accumulated at -10°C , however, indicated a greater number of bubbles per unit volume which implies that the average diameter of the air bubbles in this type of atmospheric ice is less than that of ice accumulated at -6°C .

For the ice accumulated at -10°C and -6°C the grains are elongated perpendicularly to the cylinder axis. For the ice accumulated at -20°C , however, the columnar structure is not nearly as apparent.

5. Results and discussion

Figs. 3 and 4 show the comparative results of bending strength and effective modulus of atmospheric ice accumulated at -6°C , -10°C and -20°C and tested at the same temperature. The ice accumulated at -10°C was tested at two additional temperatures (-3°C and -20°C). Flexural strength σ_f and effective modulus E_f have been calculated from simple elastic beam theory using the equations:

$$\sigma_f = \frac{3FL}{2wh^2} \text{ and } E_f = \frac{1}{4w} \left(\frac{L}{h} \right)^3 \frac{F}{d}$$

where F is the failure load; L is the length of the beam; w and h are width and height of the beam, respectively, measured at the failure plane; and d is the beam deflection. For a typical test the stress in the beam increased in a fairly linear fashion until failure occurred. The maximum flexural stress before failure is defined as the flexural strength of the specimen.

The results of bending tests on atmospheric ice accumulated at -10°C in Fig. 3 show a clear dependency of bending strength on test temperature for the three lower strain rates. This trend of increasing strength with decreasing temperature has also been reported by Gagnon and Gammon (1995) for iceberg ice and Gow and Ueda (1988) for freshwater ice.

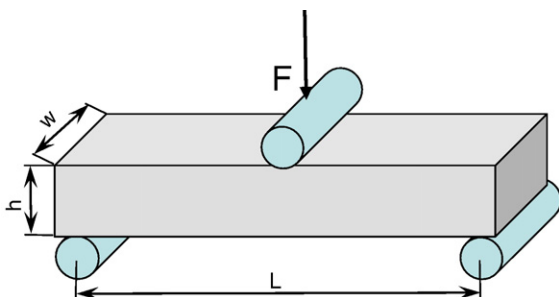


Fig. 2. Specimen dimensions in bending tests.

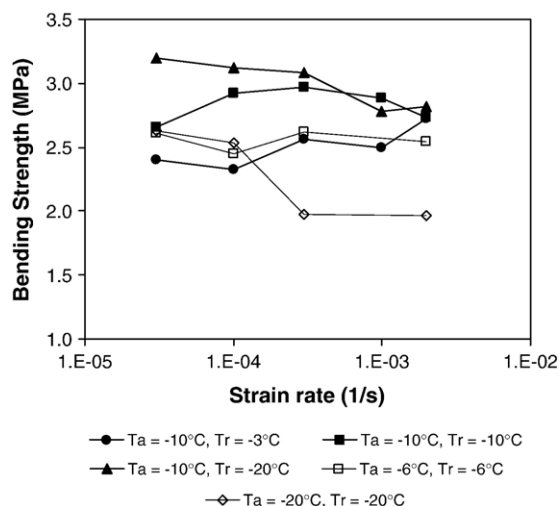


Fig. 3. Bending strength of atmospheric ice accumulated and tested at various temperatures. (Ta= Accumulation temperature; Tr= Test temperature). The standard errors for the points on the graph range from 0.07 to 0.37 MPa.

The average flexural strength of atmospheric ice accumulated at -10°C and tested at the same temperature at a strain rate of 10^{-4}s^{-1} has been calculated to be $2.92 \pm 0.26\text{MPa}$. So far, to the best of our knowledge, there is no published investigation of the flexural strength of atmospheric ice with which to compare our results. In comparison with freshwater ice, however, Timco and Frederking (1982) reported the bending strength of freshwater ice to be $2.20 \pm 0.32\text{MPa}$ and $1.77 \pm 0.19\text{MPa}$ for three-point beam bending, at approximately the same strain rate, with top and bottom in tension, respectively. Dempsey et al. (1989), in their tests by four-point-bend beams obtained a bending strength for freshwater ice ranging between 1.5MPa and 1.7MPa and between 1.2MPa and 1.7MPa for the smaller and larger beams, respectively.

The average flexural strength of this type of atmospheric ice at the test temperature of -10°C at a strain rate of $2 \times 10^{-3}\text{s}^{-1}$ has been found to be $2.74 \pm 0.59\text{MPa}$ in our study. Gow and Ueda (1988) reported values of $2.41 \pm 0.29\text{MPa}$ and $1.59 \pm 0.17\text{MPa}$ at -10°C for the three-point beam with top and bottom in tension, respectively.

The average flexural strength of this type of atmospheric ice at -3°C at a strain rate of $2 \times 10^{-3}\text{s}^{-1}$ has been found to be $2.73 \pm 0.31\text{MPa}$. Lavrov (1971) reported an average bending strength for freshwater ice of approximately 2.01MPa for S1 ice and 2.16MPa for S2 ice tested at -3°C to -4°C . Gow and Ueda (1988) reported values of $2.10 \pm 0.39\text{MPa}$ and $1.39 \pm 0.27\text{MPa}$ for S1 ice tested at -5°C with top and bottom in tension, respectively.

At a test temperature of -20°C , for ice accumulated at -10°C the average bending strength at the strain rate of $2 \times 10^{-3}\text{s}^{-1}$ has been found to be $2.82 \pm 0.46\text{MPa}$. Gow and Ueda (1988) reported a similar value of $2.57 \pm 0.29\text{MPa}$ and $1.64 \pm 0.12\text{MPa}$ at -19°C for the three-point-beams with top and bottom in tension, respectively. Fig. 5 shows the comparison between the present values of flexural strength of atmospheric ice (at strain rate of $2 \times 10^{-3}\text{s}^{-1}$) and those of other investigators for freshwater ice and glacier ice. Higher values of flexural strength of atmospheric ice can be attributed to the lower average grain size in comparison with the ice of other studies.

Timco and O'Brien (1994) reviewed the results of many researchers on the flexural strength of freshwater ice and sea ice for both cantilever and simply supported beam tests. According to their research, the flexural strength of freshwater ice lies within a range of 1MPa to 3MPa.

At a test temperature of -10°C and strain rate of $2 \times 10^{-3}\text{s}^{-1}$, the average effective modulus of atmospheric ice accumulated at -10°C has been found to be $1.06 \pm 0.17\text{GPa}$. Timco and Frederking (1982) reported the effective modulus of freshwater ice of cantilever beams to be $1.6 \pm 0.4\text{GPa}$. Gow and Ueda (1988) reported a similar value of $6.0 \pm 1.5\text{GPa}$ and $6.4 \pm 1.2\text{GPa}$ for three-point-beams of freshwater ice in bottom and top in tension, respectively. Dempsey et al. (1989) obtained the effective modulus of freshwater ice ranging between 0.7GPa and 2GPa and between 2.5GPa and 10.5GPa for smaller and larger beams, respectively, for four-point-bending experiments.

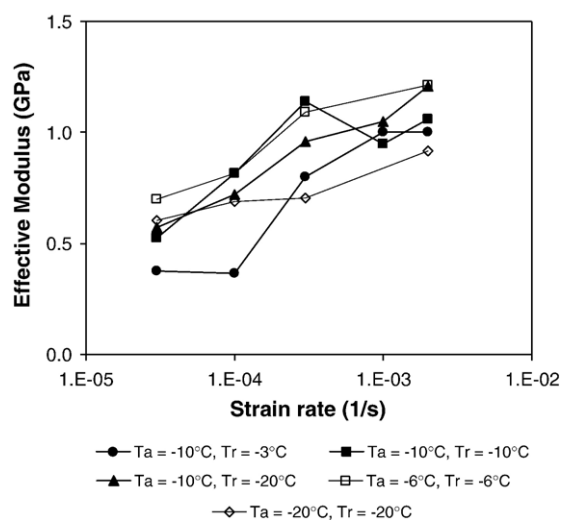


Fig. 4. Effective modulus of atmospheric ice accumulated and tested at various temperatures. The standard errors for the points on the graph range from 0.03 to 0.19 MPa.

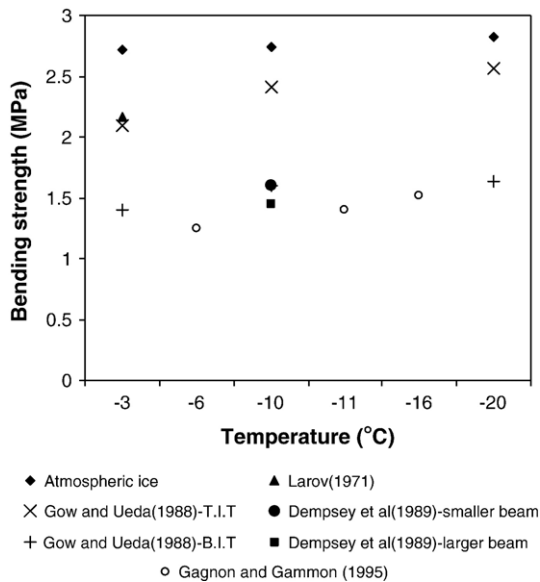


Fig. 5. Comparison of bending strength of atmospheric ice with values of other researchers for fresh water ice and glacier ice. (T.I.T=Top In Tension; B.I.T=Bottom In Tension).

The average effective modulus of this type of atmospheric ice at $-3\text{ }^{\circ}\text{C}$ at a strain rate of $2 \times 10^{-3}\text{ s}^{-1}$ is $1.01 \pm 0.18\text{ GPa}$. Gow and Ueda (1988) reported a value of $5.9 \pm 0.7\text{ GPa}$ and $6.4 \pm 1.0\text{ GPa}$ at a test temperature of $-5\text{ }^{\circ}\text{C}$ with top and bottom in tension beam tests, respectively. Lavrov (1971) reported an effective modulus of about 2 GPa at a test temperature of $-5\text{ }^{\circ}\text{C}$.

At a test temperature of $-20\text{ }^{\circ}\text{C}$ and a strain rate of $2 \times 10^{-3}\text{ s}^{-1}$, for ice accumulated at $-10\text{ }^{\circ}\text{C}$, the average effective modulus of ice has been found to be $1.21 \pm 0.26\text{ GPa}$. Gow and Ueda (1988) reported values of $8.3 \pm 2.3\text{ GPa}$ and $7.9 \pm 0.9\text{ GPa}$ at $-19\text{ }^{\circ}\text{C}$ for three-point-beam bending tests with top and bottom in tension, respectively. Fig. 6 shows the comparison between the present values of effective modulus of atmospheric ice (again accumulated at $-10\text{ }^{\circ}\text{C}$ and tested at a strain rate of $2 \times 10^{-3}\text{ s}^{-1}$) and those of other investigators for freshwater ice.

In Figs. 3 and 4, it is observed that the bending strength and the effective modulus of atmospheric ice accumulated at $-20\text{ }^{\circ}\text{C}$ and tested at the same temperature are lower than the values for the two other types tested at their accumulation temperatures. The reasons for these differences will be discussed in the following paragraphs.

In Fig. 3, it can be observed that at the lower strain rates, the strength of the ice accumulated at $-10\text{ }^{\circ}\text{C}$ appears to increase with decreasing temperature, as expected. Unfortunately, there are no other data in the literature to compare this trend to for the low strain rates. On the other hand, Fig. 3 suggests little or no temperature

effect at the higher strain rates for this type of atmospheric ice. Gagnon and Gammon (1995) noticed an increasing trend in flexural strength with decreasing temperature at a strain rate of 10^{-3} s^{-1} for iceberg ice. Gow and Ueda (1988) also observed that increasing trend at a similar strain rate.

From the trends observed in Fig. 3 for the ice accumulated at $-10\text{ }^{\circ}\text{C}$, bearing in mind the inherent scatter in the data, the implication is that strain rate and temperature affect the flexural strength of the ice in a small but measurable way. Depending on the temperature, increasing strain rate can either increase or decrease the flexural strength. Again, there is not much in the literature allowing us to make comparisons, but Gagnon and Gammon (1995) also observed that strain rate has an effect on flexural strength, for iceberg ice specimens whose strength increased with strain rate at $-11\text{ }^{\circ}\text{C}$. While Timco and Frederking (1982) stated that no distinct loading rate effect could be found in their study of the flexural strength of freshwater ice, their data (Fig. 3 in their paper) nevertheless show a statistically significant increase in strength with loading rate for simply supported beams with bottom failure, even over the limited range of the loading rates used for the tests. Furthermore, their cantilever beam tests showed a statistically significant decrease in strength with loading rate over a wider range of loading rates. This discussion shows that the relationship of the flexural strength of ice with respect to temperature and strain rate is not fully understood and warrants further study.

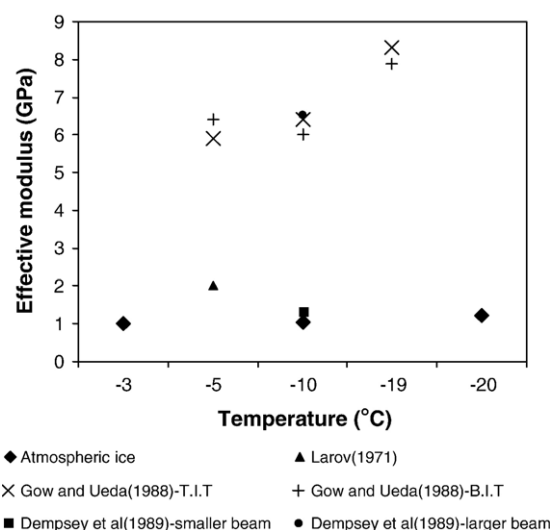


Fig. 6. Comparison of effective modulus of atmospheric ice with values of other researchers for fresh water ice. (T.I.T=Top In Tension; B.I.T=Bottom In Tension).

As shown in Fig. 3, the bending strength of the ice accumulated at $-10\text{ }^{\circ}\text{C}$ is higher than that of the two other ice types. The smaller grain size of this ice, as compared to that of ice accumulated at $-6\text{ }^{\circ}\text{C}$, as well as the colder test temperature ($-10\text{ }^{\circ}\text{C}$) explain its higher bending strength. The similar values obtained for bending strength of ice accumulated at $-10\text{ }^{\circ}\text{C}$ and tested at $-3\text{ }^{\circ}\text{C}$ and that of ice accumulated at $-6\text{ }^{\circ}\text{C}$ and tested at $-6\text{ }^{\circ}\text{C}$, despite the warmer test temperature of the former, further demonstrates that the bending strength of atmospheric ice accumulated at $-10\text{ }^{\circ}\text{C}$ is higher than that accumulated at $-6\text{ }^{\circ}\text{C}$.

The lack of cavities and pre-existing cracks in the ice accumulated at $-10\text{ }^{\circ}\text{C}$ compared to that at $-20\text{ }^{\circ}\text{C}$, despite the warmer test temperature, results in a stronger structure and higher bending strength for the former. The significant number of cavities, many that have irregular shapes, contribute to the lower strength observed for ice accumulated at $-20\text{ }^{\circ}\text{C}$ because these cavities are susceptible to stress concentration. It can be seen in Fig. 3 that the average values of bending strength for the ice accumulated at $-10\text{ }^{\circ}\text{C}$ and tested at $-20\text{ }^{\circ}\text{C}$ are greater than the corresponding values for the ice accumulated at $-20\text{ }^{\circ}\text{C}$ and tested at the same temperature.

The difference between the bending strengths of ice accumulated at $-20\text{ }^{\circ}\text{C}$ and the other two types is more noticeable at higher strain rates. This is probably due to the stress around the tips of pre-existing cracks in the ice accumulated at $-20\text{ }^{\circ}\text{C}$. This stress increases rapidly causing crack growth before it is dissipated by plastic processes. In Fig. 3, the bending strength of the ice accumulated at $-20\text{ }^{\circ}\text{C}$ and tested at the lowest strain rate ($3 \times 10^{-5}\text{ s}^{-1}$) is almost the same as that of the ice accumulated at the other temperatures.

Fig. 4 shows that the effective modulus of all the three types of atmospheric ice increases as strain rate increases. This implies that the ratio of “load at failure” to “beam deflection at failure” (F/d) increases with higher strain rates. This is logical because at a given failure load, beam deflection at low strain rates is higher than at high strain rates. As expected, the effective modulus of ice accumulated at $-20\text{ }^{\circ}\text{C}$ at higher strain rates is less than that of the two other types, owing to the presence of cavities and cracks in this ice. The effective modulus of ice accumulated at $-6\text{ }^{\circ}\text{C}$ is higher than that at $-20\text{ }^{\circ}\text{C}$ because the larger grain size and lack of cavities in the ice accumulated at $-6\text{ }^{\circ}\text{C}$ make it less deformable (Schulson, 2001).

Furthermore, in spite of the considerable scatter in the data, the effective modulus of the ice accumulated at $-6\text{ }^{\circ}\text{C}$ is probably higher than that of the ice accumulated at $-10\text{ }^{\circ}\text{C}$. This is so because the values for the ice

accumulated at $-6\text{ }^{\circ}\text{C}$ were greater than or equal to those for the ice accumulated at $-10\text{ }^{\circ}\text{C}$ throughout the range of strain rates, including the additional data point at $1 \times 10^{-3}\text{ s}^{-1}$ for the ice grown at $-10\text{ }^{\circ}\text{C}$. This is due to the larger grain size of the ice accumulated at $-6\text{ }^{\circ}\text{C}$, relative to that of the ice accumulated at $-10\text{ }^{\circ}\text{C}$.

The difference between the results of the present study and those of other investigators for bending strength and effective modulus of freshwater ice emanates from two sources. The most important difference is the ice type. There are lots of dissimilarities between atmospheric ice and freshwater ice. The differences in grain size, void ratio, shape and size of bubbles and grain growth direction are some examples.

As mentioned earlier, the average grain size for atmospheric ice accumulated at $-10\text{ }^{\circ}\text{C}$ and $-6\text{ }^{\circ}\text{C}$ is 0.5 mm and 1.5 mm, respectively. In the tests of Gow and Ueda (1988) and those of Timco and Frederking (1982), however, the average grain size was found to be between 4 mm to 8 mm and 1 mm to 6 mm, respectively.

The other important difference between our tests and those of other researchers is the test sample size which can affect mechanical properties (Dempsey et al., 1989). The specimen dimensions in our study were 40 mm wide, 20 mm thick and 70 mm long. Timco and Frederking (1982) used sample sizes of 60 mm \times 100 mm \times 400 mm in their study. The height and width of the samples used by Gow and Ueda (1988) were in a range of 78 mm to 140 mm and the average beam length was between 710 mm and 1020 mm. The large difference in sample size between the present study and the previous ones is likely responsible for some of the differences in the results. The inherent scatter of the test results may also have contributed to the differences (e.g. see effective modulus in Dempsey et al., 1989).

6. Conclusions

More than 120 tests were carried out to measure the bending strength and effective modulus of atmospheric ice. The ice has been accumulated on a rotating cylinder in the CIGELE atmospheric icing wind tunnel at LWC of 2.5 g/m^3 , wind speed of 10 m/s and various temperatures. The ice which was accumulated at $-10\text{ }^{\circ}\text{C}$ was tested at $-3\text{ }^{\circ}\text{C}$, $-10\text{ }^{\circ}\text{C}$ and $-20\text{ }^{\circ}\text{C}$. The accumulated ice at $-6\text{ }^{\circ}\text{C}$ and $-20\text{ }^{\circ}\text{C}$ was tested at the same temperature as accumulated. The results of these tests are summarized as follows. At the lower strain rates the strength of the ice increases with decreasing temperature but no temperature effect is seen at the higher strain rates. It is also observed that,

depending on the temperature, increasing the strain rate can increase or decrease the ice strength. In view of these observations, the flexural strength behaviour of ice with respect to temperature and strain rate needs further investigation. The bending strength of atmospheric ice accumulated at $-10\text{ }^{\circ}\text{C}$ has been found to be higher than that of the two other types of atmospheric ice due to its stronger structure owing to its smaller grain size and its relative lack of cavities. Also, it has been found that the bending strength of atmospheric ice accumulated at $-20\text{ }^{\circ}\text{C}$ decreases with increasing strain rates. The effective modulus of atmospheric ice has been found to increase with increasing strain rates. At higher strain rates for the ice accumulated at $-20\text{ }^{\circ}\text{C}$ and tested at the same temperature, the effective modulus is less than the two other ice types. Owing to structural differences between atmospheric and freshwater ice, and also to differences in grain size and specimen dimensions in previous studies, some differences between our results and those of other researchers on freshwater ice have been observed and discussed.

Acknowledgements

This work was carried out within the framework of the NSERC/Hydro-Quebec/UQAC Industrial Chair on Atmospheric Icing of Power Network Equipment (CIGELE) and the Canada Research Chair on Engineering of Power Network Atmospheric Icing (INGIVRE) at Université du Québec à Chicoutimi. The authors would like to thank the CIGELE partners (Hydro-Québec, Hydro One, Électricité de France, Alcan Cable, K-Line Insulators, CQRDA and FUQAC) whose financial support made this research possible.

References

- Dempsey, J.P., Wei, Y., DeFranco, S., Ruben, R., Frchetti, R., 1989. Fracture toughness of S2 columnar freshwater ice: crack length and specimen size effects — Part I. The Eighth International Conference on Offshore Mechanics and Arctic Engineering. ASME, New York, pp. 83–89.
- Druetz, J., Laforte, J.L., Tremblay, C., 1989. Experimental results on the tensile strength of atmospheric ice. The American Society of Mechanical Engineers, 8th International Conference on Offshore Mechanics and Arctic Engineering Hague, Netherlands, pp. 405–410. Book no 10285 D.
- Druetz, J., Nguyeh, D.D., Lavoie, Y., 1986. Mechanical properties of atmospheric ice. *Cold Regions Science and Technology* vol. 13, 67–74.
- Eskandarian, M., 2005. Ice shedding from overhead electrical lines by mechanical breaking, Ph.D. thesis, University of Quebec at Chicoutimi.
- Frederking, R.M.W., Svec, O.J., 1985. Stress-relieving techniques for Cantilever Beam tests in an ice cover. *Cold Regions Science and Technology* vol. 11, 247–253.
- Gagnon, R.E., Gammon, P.H., 1995. Characterization and flexural strength of iceberg and glacier ice. *Journal of Glaciology* vol. 41 (137), 103–111.
- Gow, J.A., Ueda, T.H., 1988. Structure and temperature dependence of the flexural properties of laboratory freshwater ice sheets. *Cold Regions Science and Technology* vol. 16, 249–269.
- Karev, A. R., Farzaneh, M., Kollar, L. E., submitted for publication, An Icing Wind Tunnel Study on Characteristics of an Artificial Aerosol Cloud, Part II: Liquid Water Content as a Function of Air Speed, *J. of Atmospheric and Oceanic Technology*.
- Kermani, M., Farzaneh, M., Gagnon, R.E., 2007. Compressive strength of atmospheric ice. *Cold Regions Science and Technology* vol. 49, 195–205.
- Lavrov, V.V., 1971. Deformation and strength of ice. Transl. from Russian, Natl. Sci. Found., Israel Program for Scientific Translation, Jerusalem, pp. 1–164.
- Mousavi, M., 2003. Experimental and theoretical verification of two icing codes, Thesis, University of Quebec at Chicoutimi.
- Schulson, E.M., 2001. Brittle failure of ice. *Engineering Fracture Mechanics* 68, 1839–1887.
- Schwarz, J., Frederking, R., Gavrilov, R., Petrov, I., Hirayama, K., Mellor, M., Tryde, P., Vaudrey, K., 1981. testing methods for measuring mechanical properties of ice. *Cold Regions Science and Technology* vol. 4, 245–253.
- Stallabrass, J.R., 1978. An appraisal of the single rotating cylinder method of liquid water content measurement. National Research Council of Canada, Division of Mechanical Engineering, Rep. LTR-LT-92.
- Timco, G.W., Frederking, R.M.W., 1982. Comparative strengths of freshwater ice. *Cold Regions Science and Technology* vol. 6, 21–27.
- Timco, G.W., O'Brien, S., 1994. Flexural strength equation for sea ice. *Cold Regions Science and Technology* vol. 22, 285–298.
- Timoshenko, S., 1968. Elements of Strength of Materials, 5th ed. Van Nostrand, Princeton.